Human Placental Mesenchymal Stem Cell Therapy Restores the Cytokine Efflux and Insulin Signaling in the Skeletal Muscle of Obesity-induced Type 2 Diabetes Rat Model



RESEARCH ARTICLE



Human placental mesenchymal stromal cell therapy restores the cytokine efflux and insulin signaling in the skeletal muscle of obesity-induced type 2 diabetes rat model

Nagasuryaprasad Kotikalapudi¹ · Samuel Joshua Pragasam Sampath¹ · Sukesh Narayan Sinha² · R. Bhonde^{3,4} · Sathish Kumar Mungamuri² · Vijayalakshmi Venkatesan¹

Received: 1 July 2021 / Accepted: 14 December 2021 © The Author(s) under exclusive licence to Japan Human Cell Society 2021

Abstract

Obesity poses a significant risk factor for the onset of metabolic syndrome with allied complications, wherein mesenchymal stem cell therapy is seen as a promising treatment for obesity-induced metabolic syndrome. In the present study, we aim to explore the beneficial effects of the human placental mesenchymal stromal cells (P-MSCs) on obesity-associated insulin resistance (IR) including inflammation. To understand this, we have analyzed the peripheral blood glucose, serum insulin levels by ELISA, and the glucose uptake capacity of skeletal muscle by a 2-NBDG assay using flow cytometry in WNIN/GR-Ob rats treated with and without P-MSCs. Also, we have studied insulin signaling and cytokine profile in the skeletal muscle by western blotting, dot blotting, and Multiplex-ELISA techniques. The skeletal muscle of WNIN/GR-Ob rats demonstrates dysregulation of cytokines, altered glucose uptake vis-a-vis insulin signaling. However, P-MSCs' treatment was effective in WNIN/GR-Ob rats as compared to its control, to restore HOMA-IR, re-establishes dysregulated cytokines and PI3K-Akt pathway in addition to enhanced Glut4 expression and glucose uptake studied in skeletal muscle. Overall, our data advocate the beneficial effects of P-MSCs to ameliorate inflammatory milieu, improve insulin sensitivity, and normalize glucose homeostasis underlining the Ob-T2D conditions, and we attribute for immunomodulatory, paracrine, autocrine, and multipotent functions of P-MSCs.

 $\textbf{Keywords} \ \ Human \ placental \ mesenchymal \ stromal \ cells \cdot WNIN/GR-Ob \ rats \cdot Skeletal \ muscle \ tissue \cdot Cytokines \cdot Insulin \ signaling \cdot Glut4$

Published online: 29 January 2022

- Division of Cell and Molecular Biology, ICMR-National Institute of Nutrition, Jamai-Osmania P.O., Tarnaka, Hyderabad 500007, India
- Division of Food Safety, ICMR-National Institute of Nutrition, Jamai-Osmania P.O., Tarnaka, Hyderabad 500007, India
- Department of Regenerative Medicine, Manipal Institute of Regenerative Medicine, GKVK Post, Bellary Road, Allalasandra, Yelahanka, Bangalore 560065, India
- Present Address: Dr D. Y. Patil Vidyapeeth, Pune 411018, India

Introduction

Metabolic syndrome (MS), constituting a triad of obesity, diabetes, and cardiovascular disease (CVD), has been the leading cause of death globally, both in developed and developing countries [1]. Among various causative factors, changes in lifestyle, food habits, environmental, genetic, and, more recently, epigenetic alterations are critical factors in inducing MS. In the etiology of Obesity-Induced Type2 Diabetes, one progresses from regular to impaired glucose tolerance (IGT) toT2D.

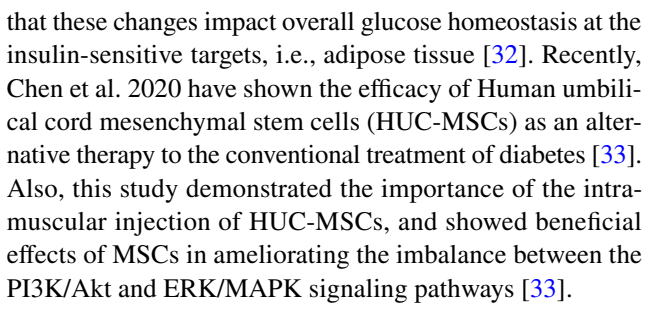
WNIN/GR-Ob rat model (WNIN mutant Obese rats) used in the present study has been indigenously developed at ICMR-NIN in the year 2011. This strain is maintained through the mating of fertile heterozygous carriers (±) and is named WNIN/Ob to indicate its origin. These rats maintain a strict Mendelian ratio during their propagation, wherein one-fourth of the progeny (recessive phenotype) is



observed in each cross between the WNIN/Ob and WNIN/GR [2–4]. WNIN/GR-Ob rats closely resemble pre-clinical /clinical obese diabetic subjects presenting with metabolic dysfunctions like IGT, insulin resistance (IR), decrease in lean body mass, osteoarthritis, hypertriglyceridemia, as well as hypercholesterolemia [2, 5–8]. The impetus obtained from our earlier studies using WNIN/GR-Ob rats presented with several pathophysiological changes like inflammation, IGT, altered glucose homeostasis, adipocyte hypertrophy, and β -cell exhaustion resulting in reduced insulin sensitivity seen with age [2, 5–7, 9, 10].

Studies show that accumulation of excess free fatty acid (FFAs) under obese conditions also exacerbates for the inflammatory milieu in the insulin target tissue like skeletal muscle [11], and also reported with a high-fat-rich diet [12]. Interestingly, IR in adipose tissue presents with increased macrophage infiltration as compared to skeletal muscle, where macrophage infiltration is relatively lesser in individuals with IR a key indicator of inflammation [13, 14]. Nevertheless, it appears that cytokines coming from other organs (adipose tissue and liver) may have an important impact on the development of IR in the muscle, and show impaired IKKβ signaling, and up-regulates several inflammatory genes (NF-κB, TNF-α, IL-6, and IL-1β) to alter GLUT4 translocation and glucose uptake [15, 16]. These alterations in muscle may be associated with altered activation of PI3K, possibly due to elevations in PKC θ [17–19]. Interestingly, an acquired loss of PI3K activation in muscle is also seen as a result of a high-fat diet. Leptin increases fatty acid oxidation and decreases esterification in skeletal muscle [20, 21]. It has also been shown that in skeletal muscle of T2D subjects, the insulin-stimulated Tyr phosphorylation of Insulin substrate receptor 1 is impaired by high levels of FFAs, which has not been evidenced in normal or in non-obese T2D [22-24]. This impairment in the signaling mechanism leads to defective or altered GLTU4 translocation to the cell membrane. Additionally, Akt activation is also impaired in T2D patients [22]. This appears to be due, at least in part, to the regulation of the expression of genes involved in fatty acid metabolism and may be exerted directly at the level of the target tissues, as the effects are seen in muscle and islets exposed to leptin ex vivo. However, enhanced signaling through the TLR-4 receptor by saturated fatty acids can reduce fatty acid oxidation of the lipids in the muscle [25, 26].

It is encouraging from the recent studies that mesenchymal stromal cell (MSC) therapy shows promising results for the treatment of T2D and associated complications [27–29]. MSC therapy improves pancreas regeneration, decreases IR, and activates progenitors to convert into β -cells [30, 31]. Also, our recent studies of Kotikalapudi et al., 2021 show that the P-MSCs injection into the right thigh region of the Obese rats decreased significantly the inflammation at a systemic level, i.e., both at serum and tissue, and showed



However, there is a lack of detailed studies emphasizing how MSC therapy modulates cytokines and insulin signaling, specifically in skeletal muscle tissues, in obesityinduced T2D complications. We hypothesize that P-MSCs administered to skeletal muscle would negate the IR, and inflammation by activating Glut4 transportation to facilitate better insulin sensitivity and efflux. In the present study, we show that intramuscular injection of P-MSCs restores glucose uptake in the skeletal muscle of WNIN/GR-Ob rats, Our data also reinstate the beneficial effects of P-MSCs and for better cross talk to enhance peripheral blood glucose clearance and restore cytokine profile comparable to Controls in the skeletal muscle of WNIN/GR-Ob rats and regulates insulin signaling. A systemic study of the therapeutic effects of P-MSCs in the treatment of IR would facilitate our understanding of the mechanism(s) and its potential clinical application in the management of T2D.

Materials and methods

Isolation, expansion, and characterization of human P-MSCs

The chorionic plate of the placenta was exposed by stripping off the amnion. This chorionic plate was then washed with phosphate buffer saline (PBS) pH 7.2 to remove traces of cord blood. This chorionic plate of the placenta was subjected to 0.25% trypsin-EDTA digestion for 30 min at 37 °C. Isolation was carried out as previously described [34, 35]. Human P-MSCs were maintained in DMEM/F12 + 10% FBS and antibiotics (Pen-Strep, Amphotericin B, and Kanamycin) till confluence at 37 °C, 5% CO₂, and 95% relative humidity in a CO₂ incubator. Media were changed every other day for all the cultures till confluence (70–80%), trypsinized using 0.25% EDTA (passaged), and seeded into fresh tissue culture flasks in a split ratio of 1:3. Cells were maintained in culture for further analysis. For chondrogenic and osteogenic differentiation, 1×10^6 human P-MSCs/cm² (passage 3) were plated onto tissue culture flasks. Differentiations were induced by replacing the growth medium (DMEM-F12) with a chondrogenic, osteogenic, differentiation bullet kit (C-28012, Sigma-Aldrich USA, and SCR028, Merck



Millipore, USA, respectively) as per the manufacturer's instructions. Chondrogenesis was confirmed using Alcian Blue staining. The osteogenesis was confirmed by staining with Alizarin Red S. Adipogenic differentiation was briefly evaluated by adipogenic induction medium and adipogenic maintenance medium (Merck Millipore SCR020, USA), and adipogenesis was confirmed using Oil Red O Staining. All the studies have been carried out using the third passage of P-MSCs, which has also been characterized for CD-133, Stro-1, CD90, CD105, CD73, and CD34 cellular markers for P-MSCs.

Animal model and study design

We confirm that all methods were carried out in accordance with guidelines and regulations for using animals and all the animal studies were carried out in compliance with the ARRIVE guidelines. Six-month-old female WNIN/Control and WNIN/GR-Ob (Ob-T2D) rats from the inbred strain from ICMR-National Institute of Nutrition (NIN) were used (n=24) for the experiments. The rats were divided into four groups: WNIN/Control (n = 6), WNIN/Control injected with P-MSCs (n=6), WNIN/GR-Ob (Ob-T2D) rats (n=6), and WNIN/GR-Ob (Ob-T2D) rats injected with P-MSCs (n=6). All the animals received standardized chow diet nutrients %/100 g: carbohydrate 48.8, protein 21, fat 3, calcium 0.8, phosphorus 0.4, fiber 5, moisture 13, ash 8, and total energy (kcal/100 g) 306.20 g during the course of the experiments, and the experiments were done in duplicates. P-MSCs (1×10^6) were suspended in 100 µl of $1 \times \text{phosphate-buffered saline } (1 \times \text{PBS})$ and were injected intramuscularly into the right thigh of the rats, one-shot/per week × 3. The control rats received an equivalent of 100 μl of 1×PBS. The biochemical, cellular, and molecular studies were conducted at the end of 7 weeks after the 3rd P-MSCs injection unless specified.

Oral glucose and insulin tolerance test (GTT/ITT)

GTT and ITT assays were performed as described previously [36]. At the end of the 7th-week post-injection, we performed GTT and ITT after fasting the animals for 8–10 h. For GTT, the rats were infused with a 20% glucose solution (2 g of glucose/kg of body mass), and for ITT, we followed the method [37] of using the formula volume of IP glucose injection (μ l) = 10×bodyweight (g) and 0.75 IU of insulin/g body mass. The blood glucose levels were measured at 15, 30, 60, and 120 min after glucose and insulin injection. Glucose levels were measured using an ACCU-CHEK Advantage Glucometer (Roche Diagnostics GmbH, Mannheim, Germany).

Biochemical analysis

The animals were deprived of food before autopsy and sacrificed. Blood was collected by retro-orbital bleeding into the serum vacutainer. Serum was prepared by centrifuging the blood samples at 1500 rpm for 20 min at RT and stored at $-80\,^{\circ}\text{C}$ till use. At the end of the experimental duration, blood was collected under fasting conditions. Serum was separated and all parameters were estimated using a semi Bioauto analyzer (ACE Alera, USA). The biochemical studies were conducted before, and at the end of 7 weeks after the 3rd P-MSCs' injection.

Enzyme-linked immunosorbent assay

Serum insulin concentration was measured using specific ELISA kits (Mercodia, Sweden). HOMA-IR was calculated as described previously [38], and following equations were used to calculate the HOMA-IR index and HOMA- β index (HBCI): HOMA-IR index = (FBG [mmol/l] × FINS [units/l])/(22.5) and HOMA- β = (20 × FINS [units/l])/(FBG [mmol/l] – 3.5).

Real-time quantitative PCR (cytokines' markers)

The qRT-PCR analysis was performed as described earlier [39] with the following modifications. Soleus muscle was used for total RNA extraction using the Trizol reagent (DSS-Takara Biosciences, India), and cDNA synthesis was performed using the enhanced Avian Reverse Transcriptase (Sigma-Aldrich, USA) as per the manufacturer's instructions. The gene expression was analyzed using the 7500 Fast Real-Time PCR instrument (Applied Biosystems, Foster City, CA, USA). β -actin expression was used as the reference gene. The list of primers used for amplification is given in Table 1 (qRT-PCR).

Measurement of tissue cytokines (dot blot)

Dot blot was performed according to the manufacturer's instructions (Abcam, USA). Briefly, the tissue lysates and serum were incubated at 4 °C with the membrane overnight and washed with wash buffer (I and II) for $3\times$ (5 min each). The biotin-conjugated cytokines (CINC-2, CINC-3, CNTF, Fractalkine, GM-CSF, IFN- γ , IL-1 α , IL-1 β , IL-4, IL-6, IL-10, Leptin, LIX, MCP-1, MIP-3 α , β -NGF, TIMP-1, TNF- α , and VEGF) were incubated with membrane overnight at 4 °C, washed with wash buffer I and II for $3\times$ (5 min each), and incubated with HRP-conjugated Streptavidin-coated into each well. After incubation for 2 h at RT, they were washed $3\times$ (5 min each)



Table 1 Primers used for amplification

RAT F Primer CXCL2 AGGGTACAGGGGTTGTTGTG RAT R Primer CXCL2 TTTGGACGATCCTCTGAACC RAT F Primer CINC-2 CACTGCTTCTGCTGCTTCTG RAT R Primer CINC-2 TGACTTCTGTCTGGGTGCAG RAT F Primer CTNF CACCCCAACTGAAGGTGACT RAT R Primer CTNF ACCTTCAAGCCCCATAGCTT RAT F Primer Fractalkine CCAAGCAGAATGTTGGGTCT RAT R Primer Fractalkine GGCATGAATGGGTTCCTCTA RAT F Primer IL-1α GCAAAGCCTAGTGGAACCAG RAT R Primer IL-1α GCAGAAGGTGCACAGTGAGA RAT F Primer IL-1 β AGGCTTCCTTGTGCAAGTGT RAT R Primer IL-β TGAGTGACACTGCCTTCCTG RAT F Primer IL-10 GGGAAGCAACTGAAACTTCG RAT R Primer IL-10 GCTTTCGAGACTGGAAGTGG RAT F Primer LIX CGCTAATTTGGAGGTGATCC RAT R Primer LIX AGTGCATTCCGCTTTGTTTT **RAT F Primer Leptin** GAGACCTCCTCCATCTGCTG **RAT R Primer Leptin** CTCAGCATTCAGGGCTAAGG AATCCTGCCCAGTCATGAAG RAT F Primer Adiponectin RAT R Primer Adiponectin TCTCCAGGAGTGCCATCTCT RAT F Primer TNF α AGATGTGGAACTGGCAGAGG RAT R Primer TNF α CCCATTTGGGAACTTCTCCT RAT F Primer IL-6 CCGGAGAGGAGACTTCACAG RAT R Primer IL-6 ACAGTGCATCATCGCTGTTC RAT F Primer Beta-actin AGCCATGTACGTAGCCATCC RAT R Primer Beta-actin CTCTCAGCTGTGGTGGAA RAT F Primer IL-12b ACCCTCACCTGTGACAGTCC RAT R Primer IL-12b TTCTTGTGGAGCAGCAGATG RAT F Primer IL-12a AGCCATGTACGTAGCCATCC RAT R Primer IL-12a CTCTCAGCTGTGGTGGAA RAT F Primer VEGF GCCCATGAAGTGGTGAAGTT RAT R Primer VEGF ACTCCAGGGCTTCATCATTG RAT F primer GM-CSF TCCTAAATGACATGCGTGCT RAT R Primer GM-CSF GCCATTGAGTTTGGTGAGGT RAT F Primer MCP-1 ATGCAGTTAATGCCCCACTC RAT R Primer MCP-1 TTCCTTATTGGGGTCAGCAC RAT F Primer TGF-β GCAACTTGGAGGAGAACTGC RAT R Primer TGF-β GTCAGAGGCTCCAGGTCTTG

again with wash buffer I and II before imaging with the ChemiDoc.

Measurement of tissue cytokine levels by multiplexing ELISA

ELISA assays (Procaratplex multiplex kit; Invitrogen, USA, and Millipore, USA) were used to measure the serum and tissue cytokine levels. The following major proand anti-inflammatory cytokines from serum and tissue lysates (Soleus muscle) were analyzed: TNF-α, monocyte

chemotactic protein 1 (MCP-1; systemic name CCL2), IL-6, GM-CSF, IL-18, IFN- γ , Leptin, and VEGF were measured using a multiplex map (Millipore, USA). IL-1 β , IL-10, IL-12 p70, IL-13, IL-4, IP-10, TNF α , and TGF- β were analyzed by ELISA using the Procaratplex multiplex kit (Invitrogen, USA). All the multiplexing assays were performed at the end of 7 weeks post-3rd P-MSCs injection as per the manufacturer's instructions.

Glucose transport assay

Glucose transport was assessed in the skeletal muscle tissue using glucose analog, 2-deoxyglucose, as described previously [40]. At the end of 7 weeks, skeletal muscle tissue (soleus muscle) was dissected under sterile conditions and stimulated with insulin for 50 min and then incubated in Krebs–Ringer-bicarbonate (KRB) buffer containing 2-NBDG. After incubation, the assay was terminated with ice-cold KRB buffer, and subsequently, uptake was measured by a flow cytometer. The control sample, which did not have the 2-NBDG, was used to set the flow cytometer compensation and gate parameters. Each experiment was performed in triplicates at the end of 7 weeks post-3rd P-MSCs injection and was averaged for the study.

Measurement of hexokinase and pyruvate kinase activity

The Hexokinase assay was performed as described previously [41]. Briefly, 20 µg of fresh tissue lysate (soleus muscle) was added to 1 ml of reaction buffer for hexokinase (50 mM Tris HCl (Sigma-Aldrich), pH 7.5, 10 mM MgCl₂ (Sigma-Aldrich), 0.6 mM ATP (Sigma-Aldrich), 100 mM glucose (Sigma-Aldrich), 0.2 mM NADP+(Sigma-Aldrich), and 0.1 units of glucose-6-phosphate dehydrogenase (Sigma-Aldrich)). Ten units of glyceraldehyde-3-phosphate dehydrogenase (Sigma-Aldrich) per ml were added for analyzing the Hexokinase activity. The Pyruvate kinase assay was performed as previously described [41]. Briefly, 20 µg of fresh tissue lysate (soleus muscle) was added to 1 ml of reaction buffer for pyruvate kinase (50 mM Tris HCl (Sigma-Aldrich), pH 7.5, 5 mM MgCl₂ (Sigma-Aldrich), 5 mM ATP (Sigma-Aldrich), 0.2 mM NADH (Sigma-Aldrich) 100 mM KCl (Sigma-Aldrich), 5 mM Na₂HPO₄ (Sigma-Aldrich), 5 mM MgCl₂ (Sigma-Aldrich), 0.01 mM AMP (Sigma-Aldrich), 5 mM fructose-6-phosphate (Sigma-Aldrich), 5 units of triosephosphate isomerase (Sigma-Aldrich) per ml, and 1 unit of aldolase (Sigma-Aldrich) per ml was added to check the pyruvate kinase activity. A negative and positive control has been included without tissue lysate and with 0.05 units of hexokinase and pyruvate kinase in both the assays. Enzyme activities were measured and represented as the



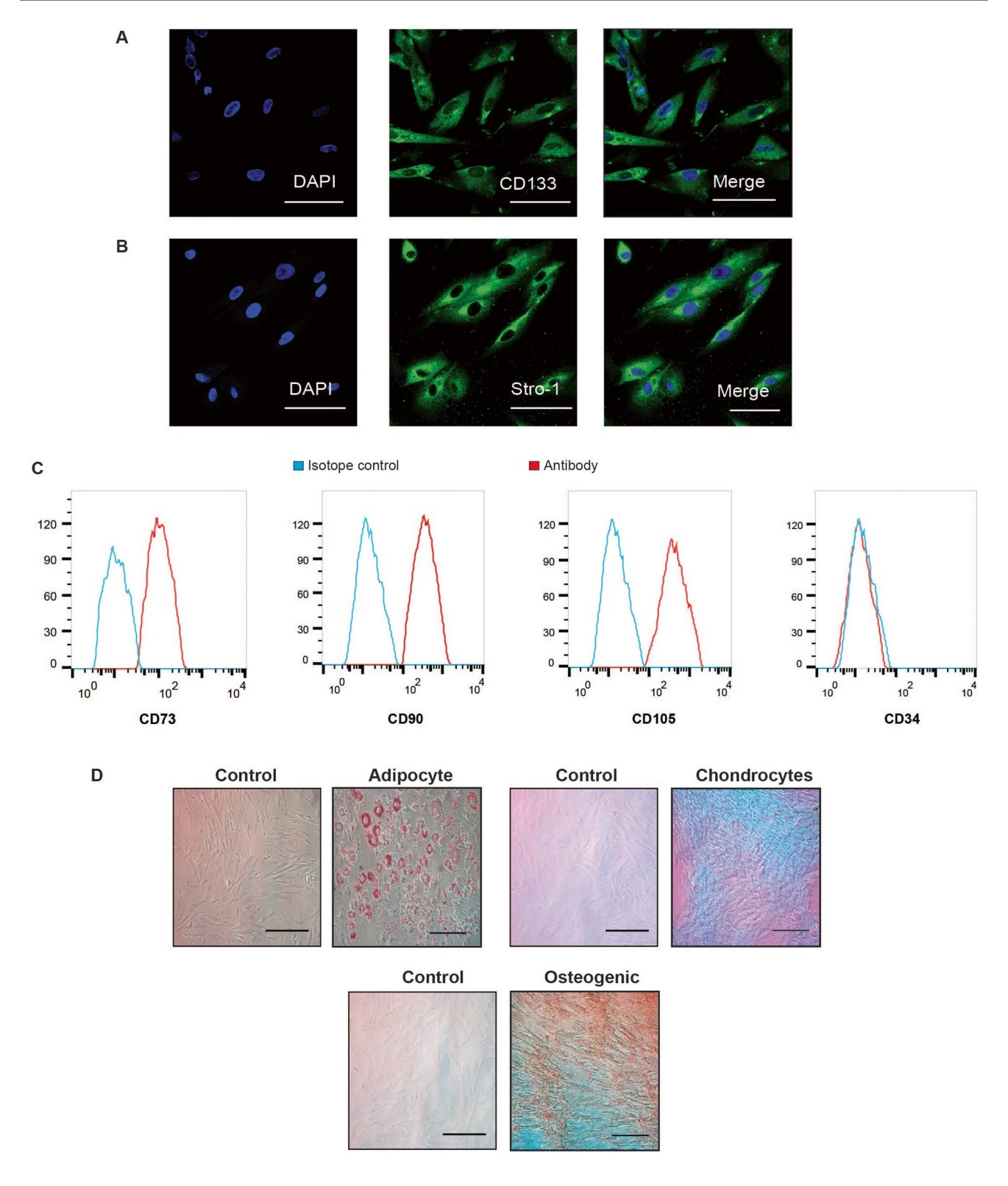
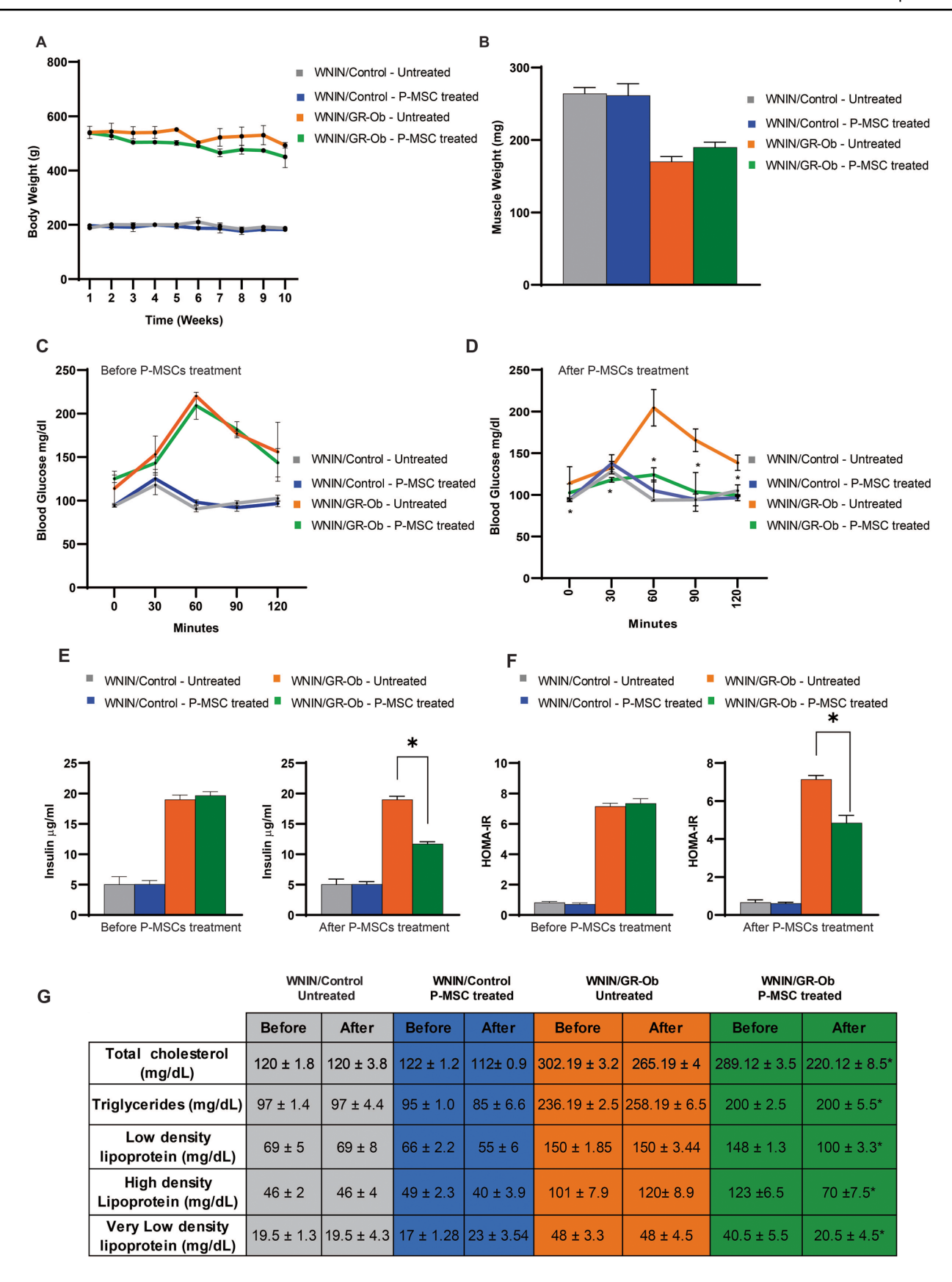


Fig. 1 Morphology, characterization of placental-derived mesenchymal stromal cells in primary cultures. **A, B** Representative confocal images of human P-MSCs stained for CD133 and Stro-1 stromal cell markers. The nuclei were stained with DAPI at 100 μM. C Flow cytometer histogram of human P-MSCs stained for CD90, CD105,

CD73, and CD34. **D** Representative microscopic images of human P-MSCs showing the Oil red, Alcian blue, and Alizarin Red staining, which are markers for adipogenic, chondrogenic, and osteogenic differentiation at $50~\mu M$







√Fig. 2 Human placental—MSCs normalize hyperglycemia and insulin sensitivity in Ob-T2D rats. A Line diagram showing the bodyweight of WNIN/Control and Ob-T2D rats during the course of the experiment. B Bar diagram indicating the total muscle weights of rats with and without P-MSCs injection. C, D Line diagram showing the glucose concentration in the peripheral blood of WNIN/Control and Ob-T2D rats, before and after the human P-MSCs injection. E Bar diagram indicating the levels of Insulin in WNIN/Control and Ob-T2D rats before and after the P-MSCs injection. F Bar diagram indicating HOMA-IR levels in WNIN/Control and Ob-T2D rats with and without human P-MSCs injection. G Total cholesterol, LDL, HDL, and VLDL levels in the blood of WNIN/Control and Ob-T2D rats before and after the human P-MSCs injection. Statistical analyses were performed between the control and the human P-MSCs injected groups, using two-way ANOVA comparing the WNIN/Control and Ob-T2D rats (*p < 0.05). Error bars represent one standard deviation from the mean. n = 6 rats per group

change in absorbance/min, calculated using a linear portion of the obtained curve.

Western blotting analysis (insulin signaling pathway)

Western blotting was performed as described previously [42]. The soleus muscle tissues were homogenized at the end of 7 weeks post-3rd P-MSCs injection. 1 X RIPA buffer containing 150 mM sodium chloride, 1% Nonidet P-40, 0.5% sodium deoxycholate, 0.1% SDS (sodium dodecyl sulfate), 50 mM Tris (pH 8.0), and protease inhibitor (Pierce) was used for homogenization. Proteins were separated by SDS-PAGE, immunoblotted with indicated antibodies, and imaged by ChemiDoc. The tissue lysates (40 µg protein/ lane) were briefly resolved by SDS-PAGE and transferred to PVDF membranes. Membranes were blocked for at least 1 h. with 4% (w/v) skim milk powder in Tris-buffered saline with 0.1% Tween 20 (TBST). The membranes were incubated overnight at 4 °C with the following primary antibodies: anti-β-actin (1:1000, mouse monoclonal, pierce), PI3K-α (1:1000, rabbit polyclonal, CST), PI3K-β (1:1000, rabbit polyclonal, CST), PI3K-γ (1:1000, rabbit polyclonal, CST), anti-AKT (1:1000, mouse monoclonal, CST), anti-P-Ser 473 AKT (1:1000, mouse monoclonal, CST), anti-P-Thr 308 AKT (1:1000, mouse monoclonal CST), anti-IRS-1 (1:1000, mouse monoclonal, CST), anti-P-Ser 307 IRS1 (1:1000, mouse monoclonal, CST), and anti-Glut4 (1:1000, mouse monoclonal, CST). Membranes were then washed three times for 15 min with TBST, and incubated for 1 h at room temperature with the respective secondary antibodies diluted 1:10,000 in 5% (w/v) skim milk powder in TBST. The membranes were rewashed three times, 15 min each with TBST, before imaging with the ChemiDoc G-Box (Syngene International limited). All the gels/blots used in the pictures complied with the digital image and integrity policies.

Statistical analysis

The results represent the mean of 6 rats per group. The "p" values were calculated using the two-way ANOVA for normally distributed data and the multiple comparison test. Statistical analysis was done using GraphPad Prism (Ver 8.0). Heatmaps were plotted using GraphPad Prism.

Results

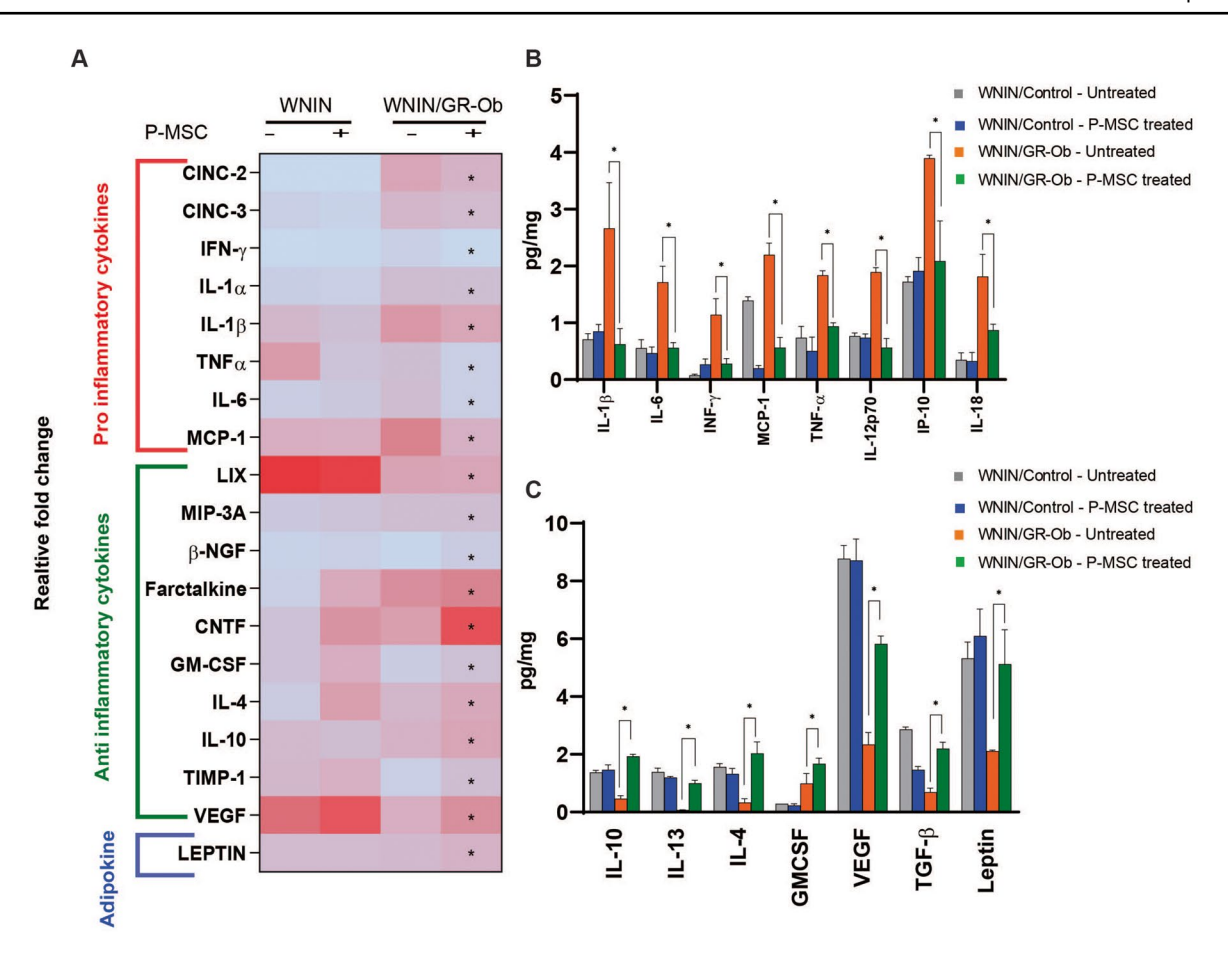
Characterization and differentiation of mesenchymal stromal cells from human placenta (P-MSCs)

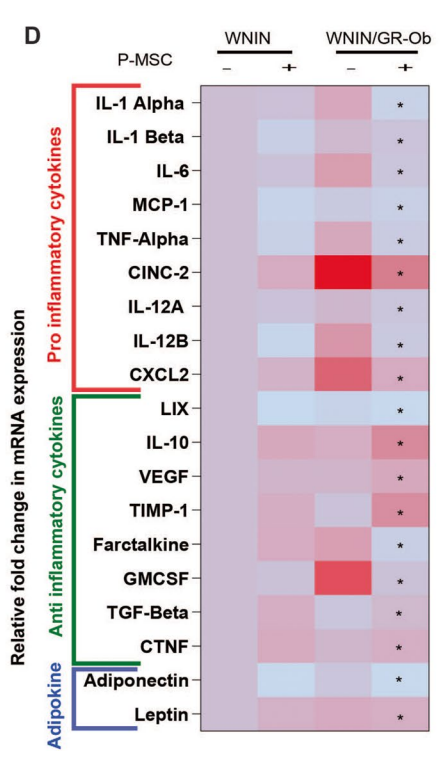
CD-133 expression is associated with stem cells, regeneration, and differentiation. CD-133 is one of the key biomarkers for the isolation and characterization of stem cells (Fig. 1A) [43] CD-133-positive cells isolated from cord blood have been studied for tissue repair both in clinical and animal model systems [44, 45]. The expression of Stro-1 (Fig. 1B) is a characteristic feature of immature precursor cells, and has been used for MSCs' isolation and identification from the umbilical cord and bone marrow tissue [46]. Koyama et al. have demonstrated that human synovial fluid expressed Stro-1 cells were capable of differentiating into several cell types, including osteoblasts, chondrocytes, and adipocytes in vitro [47]. Thus, we performed CD-133 and Stro-1 immunostaining of the human P-MSCs to confirm their multipotent lineage capability. Also, these cells stained positive for surface markers CD73, CD90, CD105, and stained negative for CD34 (Fig. 1C). To identify the multipotential ability of human P-MSCs, we performed adipogenic, chondrogenic, and osteogenic as described in the section "Materials and methods." The human P-MSCs were able to differentiate into adipogenic as indicated by Oil red O, chondrogenic as indicated by the positive staining with Alcian blue, and Osteogenic by Alizarin Red, respectively (Fig. 1D).

Human P-MSCs therapy leads to peripheral blood glucose clearance in WNIN/GR-Ob rats

To understand the beneficial effect of P-MSCs in clearing the peripheral blood glucose and restoration of insulin signaling in obese conditions. Our study showed that the WNIN/GR-Ob rats treated with P-MSCs are associated with no changes in their body weights (Fig. 2A), but there was an increase in the overall muscle weight (Fig. 2B), after the P-MSCs injection in the WNIN/GR-Ob rats when compared with the WNIN/GR-Ob Control rats.









∢Fig. 3 Human P-MSCs treatment re-establishes the cytokine expression in the skeletal muscles of Ob-T2D rats in vivo. A Dot blot heat maps showing the cytokine concentrations in each of the conditions, the intensity of the colors assigned as the mean of 6 animals from each group indicate the relative scale of expression, ranging from 0 to 40. B, C Bar diagram showing the absolute concentration of proand anti-inflammatory cytokines in the skeletal muscle of WNIN/ Control and Ob-T2D rats, with and without human P-MSCs injection, as measured by the Luminex system. D Heat maps are shown as the mean of 6 animals from each group and the relative mRNA fold change in the skeletal muscle of WNIN/Control and Ob-T2D rats with and without human P-MSCs injection. Statistical analyses were performed between the control and the human P-MSCs injected groups, using two-way ANOVA comparing the WNIN/Control and Ob-T2D rats (*p<0.05). Error bars represent one standard deviation from the mean. n=6 rats per group

Next, to understand the role of P-MSCs in clearing the peripheral blood glucose and restoration of insulin utilization in WNIN/GR-Ob rats, we performed the oral glucose tolerance test (OGTT) assay, before and after human P-MSCs injection, and compared it with the WNIN/Control rats. As shown previously [6], we also observed that the WNIN/GR-Ob rats showed decreased glucose tolerance, when compared to the WNIN/Control rats (Fig. 2C, D). OGTT assay using the peripheral blood indicated that P-MSCs treatment improved the glucose utilization in WNIN/GR-Ob rats, in comparison to the WNIN/Control rats (Fig. 2D). In addition, we have also observed that the WNIN/GR-Ob rats, in response to P-MSCs injection, showed a significant decrease in the serum insulin levels (Fig. 2E). "HOMA-IR" analysis is a widely accepted methodology for measuring IR [48]. We show that WNIN/ GR-Ob rats have a 1.09-fold decrease in the HOMA-IR levels, compared to WNIN/GR-Ob Control rats, and a sevenfold increase in the HOMA-IR levels when compared to the WNIN/control rats (Fig. 2F) is showing a similar trend as reported previously from various studies. [2, 6, 49]. Furthermore, in response to P-MSCs treatment, we also observed decreased total cholesterol, total triglycerides, LDL, HDL, and VLDL levels in the serum isolated from the WNIN/GR-Ob rats (Fig. 2G). These data confirm that de novo, human P-MSCs injection increases insulin sensitivity and enhances glucose utilization under obesogenic milieu.

Human P-MSCs treatment remodels the cytokine expression in the WNIN/GR-Ob rats in vivo

Next, we studied whether the human P-MSCs injection also leads to cytokine remodelling. We observed that human P-MSCs injection into WNIN/GR-Ob rats had restored both the pro-and anti-inflammatory cytokines, as well as Leptin expression to the extent seen in the WNIN/Control rats (Fig. 3A). We also reconfirmed the above observations that

the P-MSCs injection restores cytokine profile in the WNIN/GR-Ob rats as analyzed by Multiplex-ELISA (Fig. 3B, C). Note that this cytokine remodelling in WNIN/GR-Ob rats occurs at the transcriptional level, since we observed an alteration of these cytokines at their mRNA expression levels, in response to P-MSCs therapy (Fig. 3D).

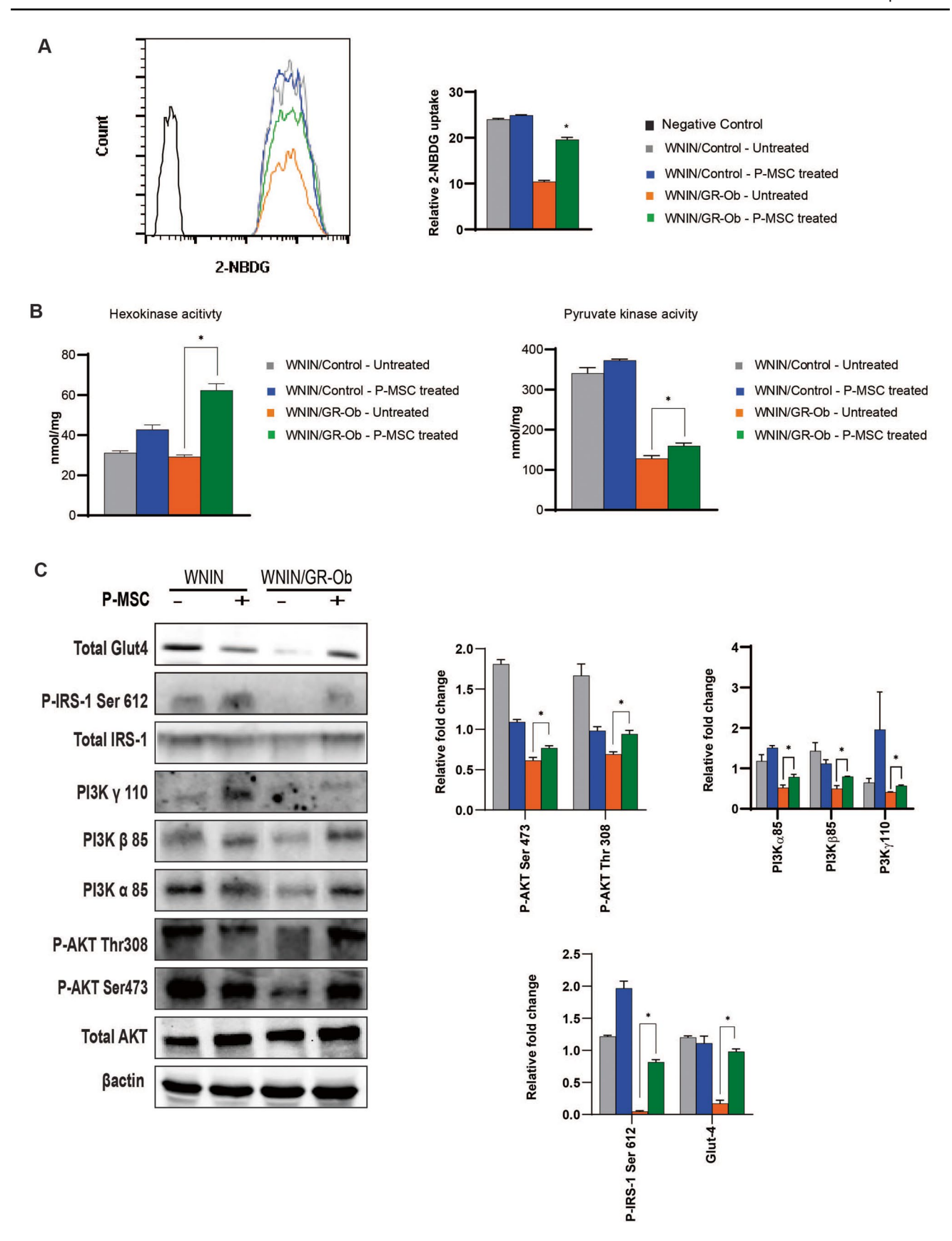
Human P-MSCs' treatment restores glucose uptake in the skeletal muscle tissues of WNIN/GR-Ob rats in vivo

Next, we analyzed whether the decrease in inflammatory milieu observed in the WNIN/GR-Ob rats to human P-MSC therapy has any impact on the glucose uptake capacity of the skeletal muscles. For this, we first isolated soleus muscle [40] from WNIN/GR-Ob rats and WNIN/Control rats and compared the respective glucose uptake capacity using 2-deoxy-2-[(7-nitro-2,1,3-benzoxadiazol-4-yl) amino]-D-glucose (2-NBDG) assay. Soleus muscle of the WNIN/GR-Ob rats had less glucose uptake capacity, compared to the WNIN/Control rats (Fig. 4A). Interestingly P-MSCs injection was more effective to WNIN/GR-Ob rats to re-establish glucose uptake ability of the soleus muscle (Fig. 4A). Corroborating with this data, we also observed an increase in the activity of Hexokinase and Pyruvate Kinase enzymes in the soleus muscle of WNIN/GR-Ob rats, compared to WNIN/Control rats (Fig. 4B).

Human P- MSCs therapy up-regulates insulin signaling and restores the Glut4 expression in skeletal muscle tissues under obesogenic milieu in vivo

Next, we investigated the insulin signaling pathway to delineate the mechanism for induced glucose uptake in the skeletal muscle of WNIN/GR-Ob rats in response to P-MSCs therapy. Immunoblotting analysis showed that P-MSCs' treatment upregulated the Ser612-IRS-1, Thr308-Akt, and Ser473-Akt phosphorylation in the skeletal muscle tissues of WNIN/GR-Ob rats' compared to WNIN/Control rats (Fig. 4C, D). Similarly, P-MSCs therapy in WNIN/GR-Ob rats had upregulated the expression of both p85 α and p85 β , which was not observed in the WNIN/Control rats (Fig. 4C, D). Interestingly, human P-MSCs injection into the WNIN/ GR-Ob rats had restored the expression of p100y in the skeletal muscle in WNIN/GR-Ob rats but not in WNIN/ Control rats (Fig. 4C, D). Note that P-MSCs treatment significantly upregulated the GLUT4 expression in WNIN/ GR-Ob rat's skeletal muscle tissues, which is comparable to that of untreated WNIN/Control rat tissues (Fig. 4C, D). These findings suggest that the increased glucose uptake in the WNIN/GR-Ob rats in the skeletal muscles is due to







√Fig. 4 Human P-MSCs therapy restores glucose uptake by upregulating PI3K-Akt signaling in the skeletal muscle tissue of Ob-T2D rats in vivo. A FACS analysis showing 2-NBDG uptake in the skeletal muscle of WNIN/Control and WNIN/GR-Ob rats treated without or with human P-MSCs and in the absence and presence of insulin stimulation. A line diagram showing the relative 2-NBDG uptake was also shown. B Bar diagrams showing Hexokinase and Pyruvate Kinase activities in the skeletal muscle of WNIN/Control and Ob-T2D rats with and without human P-MSCs injection. C Western blot analysis for the indicated proteins isolated from the skeletal muscle tissues from WNIN/Control and Ob-T2D rats with and without human P-MSCs injection. **D** Bar diagram showing the relative phosphorylation of each protein normalized to the respective total protein level. Blots are representative of four independent experiments. Statistical analyses were performed using two-way ANOVA comparing the control group and the P-MSCs injected a group of WNIN/Control and WNIN/GR-Ob (Ob-T2D) rats (*p<0.05). The error bars represent one standard deviation from the mean. n=6 rats per group

enhanced PI3K-Akt signaling-mediated Glut4 upregulation in response to P-MSCs injection.

Discussion

During T2D, there is a high glucose accumulation in the peripheral blood due to dysregulation of insulin signaling in the skeletal muscle [50], which accounts for nearly 70% of insulin-dependent glucose disposal [51]. We have shown that an intramuscular injection of P-MSCs isolated from the human placenta reduced obesity improved IR and glucose homeostasis in the adipose tissue of WNIN/GR-Ob obese rats [32]. In the present study, we further demonstrate that intramuscular injection of P-MSCs to WNIN/GR-Ob rats sensitizes their skeletal muscle tissues to the endogenous insulin and effectively counteracts the glucose imbalance, as evidenced by the normalization of HOMA-IR and OGTT levels.

We observed that the skeletal muscle of WNIN/GR-Ob rats presented with low Glut4 expression vis-a-vis leading to lower glucose uptake. Interestingly, P-MSCs injection to WNIN/GR-Ob rats increased glucose uptake by inducing the Glut4 expression in the soleus muscle in addition to enhanced glucose utilization in the skeletal muscle as evidenced by the increased activity of Hexokinase and Pyruvate Kinase enzymes. Finally, we associated these changes to glucose uptake and utilization, with normalization in the Insulin signaling pathway in the skeletal muscle of WNIN/GR-Ob rats which was promising with P-MSCs therapy.

Cytokines play a crucial role in intracellular cell signaling and function in paracrine and endocrine patterns as immunomodulating agents, modifying the balance between humoral- and cell-mediated immunity [52, 53]. The cytokines are responsible for attracting the macrophages into the surrounding milieu, causing inflammation and IR in obese patients [54]. Following the published literature [52,

53], MSCs of perinatal origin (P-MSCs) blunt the inflammatory response in target tissues. This suggests that paracrine secretions of MSCs and their cytokines/interleukin profiles (IL-6, -7, -8, -11, -12, -14, -15, -27, LIF, M-CSF, in addition to IL-10 and TGF- β 1) may play a crucial role in overcoming inflammatory responses. We also observed an increased expression of pro-inflammatory cytokines, such as IL-6, IL-1 β , and TNF- α , and a decreased expression of anti-inflammatory cytokines, such as IL-10, TGF- β , and IL-4, in the WNIN/GR-Ob rats. In the present study, we observed that the P-MSCs injection into the WNIN/GR-Ob rats had negated the expression of IL-6, TNF- α , and IL-7, -8, -11, -12, -14, -15, -27, LIF, M-CSF, in addition to IL-10 and TGF- β 1 cytokines. This advocates the potential application of human P-MSCs for the treatment of Ob-T2D.

Ob-T2D leads to a total derangement of immune functions, where both diet-induced and genetically modified obese animals show altered natural killer (NK) cell function in addition, to T-cell dysregulation [55]. Previously reported data with obese (WNIN/GR-Ob) rats showed an impaired innate immune response, i.e., increased ratio of CD4/CD8 with a dysregulation in the humoral immunity like increased levels of IgG and IgM [56, 57] vis-a-vis a reduction in the Jak2 protein expression in the WNIN/GR-Ob rats [8]. These observations reinstate that WNIN/GR-Ob rats do present with altered immunity akin to obese subjects [8].

MSCs from promising adult stem cells in regenerative therapy and have been well documented for their plasticity and multipotent functions. [58]. Indeed, it has been shown in diabetic models that P-MSCs are known to blunt the inflammatory response and allow tissue remodeling after injury [59]. Furthermore, MSCs can also suppress immune activation when exposed to pro-inflammatory cytokines such as TNF- α , INF- γ , and IL-6. We believe that interventions with MSCs to repair/restore innate and humoral immunity of the Ob-T2D rats could be attributed to the potent immunomodulatory functions of MSCs [59].

In the animal models, MSC treatment demonstrated exciting therapeutic effects on glycemic control by restoring islet function and ameliorating insulin resistance. Interestingly, studies have shown that mesenchymal stem cell therapy had alleviated insulin resistance, via promoting the conversion of macrophages from classically activated M1 macrophages (pro-inflammatory) into alternatively activated M2 macrophages (anti-inflammatory) [60, 61]. Recently, Chen et al., 2020 had showed that intramuscular injection of mesenchymal stem cells ameliorates high-fat-diet-induced diabetes and its complications, using the mice model [33]. Sun et al., 2017 showed that placental and umbilical cordderived mesenchymal stem cells had diminished insulin resistance by suppressing inflammasome-mediated inflammation in T2D rats [62]. Also, our recently published study of Kotikalapudi et al., 2021 has shown the beneficial effects



of MSCs to negate obesity-induced T2D metabolic alterations [32]. Many studies (both pre-clinical and clinical trials) show increasing evidence of the therapeutic effectiveness of MSCs. However, many studies also provide evidence of low engraftment of MSCs due to their short-lived viability after injection [63, 64]. Mäkelä et al., 2015 have shown that MSCs after intravenous transplantation were trapped in the lungs, resulting in a reduction in the MSCs' cell population at the target sites [65]. The method by which the cells are administered may be an important factor in their reaching their intended destination. Major advantages of intramuscular MSC delivery are: (a) extended time provided by dense muscle fibers that retain the MSCs in situ; (b) high vascular density that provides a conduit for the systemic release of MSC trophic factors; and (c) an abundance of tissue that provides for multiple injection sites [66]. In this study, P-MSCs injected via intramuscular route suppressed obesity-induced inflammation in insulin-targeting tissues. We presently do not know whether inflammation plays any role in P-MSCinduced decrease in hyperglycemia and hyperlipidemia seen in WNIN/GR-Ob rats.

Clinical efficacy of MSCs treatment for T2D has shown some good outcomes, where a study conducted by Estrada et al., 2008 has demonstrated that combination therapy with BM-MSC and hyperbaric oxygen therapy (HOT) were effective and reduced their glycosylated hemoglobin (HbA1c) level in T2D patients followed up to 1 year [67]. Also, another two more studies conducted by Bhansali et al., 2014 have shown that patients' dependence on insulin was decreased with BM-MSC transplantation [68, 69]. Various other clinical studies [70–75] have also shown a decrease in the HOMA-IR after MSC transplantation; however, all these studies have employed intravenous or intrapancreatic injection of MSCs into the patients. Potential risks of MSCs treatment via this route have to be considered, as the intravenous administration can cause pulmonary, upper respiratory, and immunological adverse events. In some studies, transient self-limiting nausea, vomiting, headache, abdominal pain, and upper respiratory tract infection occasionally occurred after the MSC transplantation. Currently, this is a cause of concern for the establishment and clinical application of the use of MSCs in the management of T2DM.

Based on our hypothesis, although subject to the limitations of short-term rat models, we have been able to demonstrate the functional response of P-MSCs in improving systemic and tissue inflammation, glucose tolerance, and enhancing insulin sensitivity in obese rats. These data do suggest that way forward applications of cellular therapies with P-MSCs and can be explored in T2D. However, addressing the human diabetic subjects necessitates understanding several confounding factors like duration of T2D, insulin resistance, inflammation, as well as pancreatic beta exhaustion as modifiers of response. Therefore, requires

more in-depth studies to delineate the potent beneficial functions of P-MSCs to restore normoglycemia in human subjects. Overall present study's findings using WNIN/GR-Ob rat open up newer avenues in the management strategy of obesity, diabetes, and allied complications.

Acknowledgements The authors would like to acknowledge Dr. R. Hemalatha, Director, ICMR-NIN, for providing the necessary infrastructure to conduct the current research and sanction intramural funding. We wish to thank the Animal Facility for all its support in carrying out these experiments. We also thank ICMR for the SRF manpower support.

Author contributions KN carried out most of the animal experimentation, cell, and molecular work including characterization and injection of P-MSCs. SJPS was also associated in preparation, characterization, and injection of P-MSCs into rats. SNS and SKM were involved in designing some experiments, configuration of figures, and preparation of the manuscript. RRB was involved in human placenta collection, human ethical approval, as well as isolation of P-MSCs. VV coordinated the overall team, including project design and manuscript preparation.

Funding The present study has been supported by ICMR-NIN intramural fundings (15-BS03 and 18-BS10) to Dr. VV, KN received a Senior Research Fellowship (5/3/8/31/ITR-F/2018-ITR) from ICMR for the present study.

Declarations

Conflict of interest The authors declare that there is no conflict of interest associated with this article.

Ethics statement The authors confirm that the journal's ethical policies, as noted on the journal's author guidelines page, have been adhered to, and the appropriate ethical review committee approval has been received. Institutional Animal Ethics Committees (IAECs): P35F/IAEC/NIN/11/2012/VV/WNIN. Institutional Human Ethics Committees: MHB/SCR/021.

References

- Cornier MA, Dabelea D, Hernandez TL, Lindstrom RC, Steig AJ, Stob NR, et al. The metabolic syndrome. Endocr Rev. 2008;29(7):777-822. https://doi.org/10.1210/er.2008-0024.
- Harishankar N, Vajreswari A, Giridharan NV. WNIN/GR-Ob—an insulin-resistant obese rat model from inbred WNIN strain. Indian J Med Res. 2011;134(3):320–9.
- Giridharan NV, Lakshmi CN, Raghuramulu N. Identification of impaired-glucose-tolerant animals from a Wistar inbred rat colony. Lab Anim Sci. 1997;47(4):428–31.
- Kalashikam RR, Battula KK, Kirlampalli V, Friedman JM, Nappanveettil G. Obese locus in WNIN/obese rat maps on chromosome 5 upstream of leptin receptor. PLoS ONE. 2013;8(10): e77679. https://doi.org/10.1371/journal.pone.0077679.
- Pragasam SSJ, Venkatesan V. Metabolic syndrome predisposes to osteoarthritis: lessons from model system. Cartilage. 2020. https:// doi.org/10.1177/1947603520980161.
- Singh H, Ganneru S, Malakapalli V, Chalasani M, Nappanveettil G, Bhonde RR, et al. Islet adaptation to obesity and insulin



- resistance in WNIN/GR-Ob rats. Islets. 2014;6(5–6): e998099. https://doi.org/10.1080/19382014.2014.998099.
- Madhira SL, Challa SS, Chalasani M, Nappanveethl G, Bhonde RR, Ajumeera R, et al. Promise(s) of mesenchymal stem cells as an in vitro model system to depict pre-diabetic/diabetic milieu in WNIN/GR-Ob mutant rats. PLoS ONE. 2012;7(10): e48061. https://doi.org/10.1371/journal.pone.0048061.
- Giridharan NV. Glucose & energy homeostasis: lessons from animal studies. Indian J Med Res. 2018;148(5):659–69. https://doi.org/10.4103/ijmr.IJMR_1737_18.
- Jeyakumar SM, Lopamudra P, Padmini S, Balakrishna N, Giridharan NV, Vajreswari A. Fatty acid desaturation index correlates with body mass and adiposity indices of obesity in Wistar NIN obese mutant rat strains WNIN/Ob and WNIN/GR-Ob. Nutr Metab. 2009;6:27. https://doi.org/10.1186/1743-7075-6-27.
- Jeyakumar SM, Sheril A, Vajreswari A. Vitamin A improves hyperglycemia and glucose-intolerance through regulation of intracellular signaling pathways and glycogen synthesis in WNIN/ GR-Ob obese rat model. Prev Nutr Food Sci. 2017;22(3):172–83. https://doi.org/10.3746/pnf.2017.22.3.172.
- Tumova J, Andel M, Trnka J. Excess of free fatty acids as a cause of metabolic dysfunction in skeletal muscle. Physiol Res. 2016;65(2):193–207. https://doi.org/10.33549/physiolres.932993.
- Wu H, Ballantyne CM. Skeletal muscle inflammation and insulin resistance in obesity. J Clin Investig. 2017;127(1):43–54. https://doi.org/10.1172/jci88880.
- Shoelson SE, Lee J, Goldfine AB. Inflammation and insulin resistance. J Clin Investig. 2006;116(7):1793–801. https://doi.org/10.1172/ici29069.
- Burhans MS, Hagman DK, Kuzma JN, Schmidt KA, Kratz M. Contribution of adipose tissue inflammation to the development of type 2 diabetes mellitus. Compr Physiol. 2018;9(1):1–58. https:// doi.org/10.1002/cphy.c170040.
- Mourkioti F, Rosenthal N. NF-kappaB signaling in skeletal muscle: prospects for intervention in muscle diseases. J Mol Med (Berl). 2008;86(7):747–59. https://doi.org/10.1007/s00109-008-0308-4.
- Proto JD, Tang Y, Lu A, Chen WC, Stahl E, Poddar M, et al. NF-κB inhibition reveals a novel role for HGF during skeletal muscle repair. Cell Death Dis. 2015;6(4): e1730. https://doi.org/ 10.1038/cddis.2015.66.
- da Silva Rosa SC, Nayak N, Caymo AM, Gordon JW. Mechanisms of muscle insulin resistance and the cross-talk with liver and adipose tissue. Physiol Rep. 2020;8(19): e14607. https://doi.org/10. 14814/phy2.14607.
- Griffin ME, Marcucci MJ, Cline GW, Bell K, Barucci N, Lee D, et al. Free fatty acid-induced insulin resistance is associated with activation of protein kinase C theta and alterations in the insulin signaling cascade. Diabetes. 1999;48(6):1270–4. https://doi.org/ 10.2337/diabetes.48.6.1270.
- Marrocco V, Fiore P, Madaro L, Crupi A, Lozanoska-Ochser B, Bouché M. Targeting PKCθ in skeletal muscle and muscle diseases: good or bad? Biochem Soc Trans. 2014;42(6):1550–5. https://doi.org/10.1042/bst20140207.
- Pereira S, Cline DL, Glavas MM, Covey SD, Kieffer TJ. Tissue-specific effects of leptin on glucose and lipid metabolism. Endocr Rev. 2021;42(1):1–28. https://doi.org/10.1210/endrev/bnaa027.
- 21. Muoio DM, Dohm GL, Fiedorek FT Jr, Tapscott EB, Coleman RA. Leptin directly alters lipid partitioning in skeletal muscle. Diabetes. 1997;46(8):1360–3. https://doi.org/10.2337/diab.46.8. 1360.
- 22. Pratipanawatr W, Pratipanawatr T, Cusi K, Berria R, Adams JM, Jenkinson CP, et al. Skeletal muscle insulin resistance in normoglycemic subjects with a strong family history of type 2 diabetes is associated with decreased insulin-stimulated

- insulin receptor substrate-1 tyrosine phosphorylation. Diabetes. 2001;50(11):2572–8. https://doi.org/10.2337/diabetes.50.11.2572.
- 23. Gregor MF, Hotamisligil GS. Inflammatory mechanisms in obesity. Annu Rev Immunol. 2011;29:415–45. https://doi.org/10.1146/annurev-immunol-031210-101322.
- Boucher J, Kleinridders A, Kahn CR. Insulin receptor signaling in normal and insulin-resistant states. Cold Spring Harbor Perspect Biol. 2014. https://doi.org/10.1101/cshperspect.a009191.
- Stewart CR, Stuart LM, Wilkinson K, van Gils JM, Deng J, Halle A, et al. CD36 ligands promote sterile inflammation through assembly of a Toll-like receptor 4 and 6 heterodimer. Nat Immunol. 2010;11(2):155–61. https://doi.org/10.1038/ni.1836.
- Sheedy FJ, Grebe A, Rayner KJ, Kalantari P, Ramkhelawon B, Carpenter SB, et al. CD36 coordinates NLRP3 inflammasome activation by facilitating intracellular nucleation of soluble ligands into particulate ligands in sterile inflammation. Nat Immunol. 2013;14(8):812–20. https://doi.org/10.1038/ni.2639.
- 27. Wang M, Song L, Strange C, Dong X, Wang H. Therapeutic effects of adipose stem cells from diabetic mice for the treatment of type 2 diabetes. Mol Ther. 2018;26(8):1921–30. https://doi.org/10.1016/j.ymthe.2018.06.013.
- Yaochite JN, Caliari-Oliveira C, de Souza LE, Neto LS, Palma PV, Covas DT, et al. Therapeutic efficacy and biodistribution of allogeneic mesenchymal stem cells delivered by intrasplenic and intrapancreatic routes in streptozotocin-induced diabetic mice. Stem Cell Res Ther. 2015;6(1):31. https://doi.org/10.1186/ s13287-015-0017-1.
- Si Y, Zhao Y, Hao H, Liu J, Guo Y, Mu Y, et al. Infusion of mesenchymal stem cells ameliorates hyperglycemia in type 2 diabetic rats: identification of a novel role in improving insulin sensitivity. Diabetes. 2012;61(6):1616–25. https://doi.org/10.2337/ db11-1141.
- Venkatesan V, Chalsani M, Nawaz SS, Bhonde RR, Challa SS, Nappanveettil G. Optimization of condition(s) towards establishment of primary islet cell cultures from WNIN/Ob mutant rat. Cytotechnology. 2012;64(2):139–44. https://doi.org/10.1007/s10616-011-9409-y.
- Venkatesan V, Gopurappilly R, Goteti SK, Dorisetty RK, Bhonde RR. Pancreatic progenitors: the shortest route to restore islet cell mass. Islets. 2011;3(6):295–301. https://doi.org/10.4161/isl.3.6. 17704.
- 32. Kotikalapudi N, Sampath SJP, Sukesh Narayan S, Ramesh RB, Nemani H, Mungamuri SK, et al. The promise(s) of mesenchymal stem cell therapy in averting preclinical diabetes: lessons from in vivo and in vitro model systems. Sci Rep. 2021;11(1):16983. https://doi.org/10.1038/s41598-021-96121-0.
- Chen G, Fan XY, Zheng XP, Jin YL, Liu Y, Liu SC. Human umbilical cord-derived mesenchymal stem cells ameliorate insulin resistance via PTEN-mediated crosstalk between the PI3K/Akt and Erk/MAPKs signaling pathways in the skeletal muscles of db/ db mice. Stem Cell Res Ther. 2020;11(1):401. https://doi.org/10. 1186/s13287-020-01865-7.
- 34. Mathew SA, Chandravanshi B, Bhonde R. Hypoxia primed placental mesenchymal stem cells for wound healing. Life Sci. 2017;182:85–92. https://doi.org/10.1016/j.lfs.2017.06.016.
- Mathew SA, Bhonde RR. Omega-3 polyunsaturated fatty acids promote angiogenesis in placenta derived mesenchymal stromal cells. Pharmacol Res. 2018;132:90–8. https://doi.org/10.1016/j. phrs.2018.04.002.
- Roman EA, Reis D, Romanatto T, Maimoni D, Ferreira EA, Santos GA, et al. Central leptin action improves skeletal muscle AKT, AMPK, and PGC1 alpha activation by hypothalamic PI3K-dependent mechanism. Mol Cell Endocrinol. 2010;314(1):62–9. https://doi.org/10.1016/j.mce.2009.08.007.
- Wong N, Fam BC, Cempako GR, Steinberg GR, Walder K, Kay TW, et al. Deficiency in interferon-gamma results in reduced



- body weight and better glucose tolerance in mice. Endocrinology. 2011;152(10):3690–9. https://doi.org/10.1210/en. 2011-0288.
- Lecube A, Hernández C, Genescà J, Simó R. Proinflammatory cytokines, insulin resistance, and insulin secretion in chronic hepatitis C patients: a case-control study. Diabetes Care. 2006;29(5):1096–101. https://doi.org/10.2337/diacare.2951096.
- Mungamuri SK, Qiao RF, Yao S, Manfredi JJ, Gu W, Aaronson SA. USP7 enforces heterochromatinization of p53 target promoters by protecting SUV39H1 from MDM2-mediated degradation. Cell Rep. 2016;14(11):2528–37. https://doi.org/10.1016/j.celrep. 2016.02.049.
- Chen Q, Rong P, Zhu S, Yang X, Ouyang Q, Wang HY, et al. Targeting RalGAPα1 in skeletal muscle to simultaneously improve postprandial glucose and lipid control. Sci Adv. 2019;5(4):eaav4116. https://doi.org/10.1126/sciadv.aav4116.
- TeSlaa T, Teitell MA. Techniques to monitor glycolysis. Methods Enzymol. 2014;542:91–114. https://doi.org/10.1016/b978-0-12-416618-9.00005-4.
- Mungamuri SK, Wang S, Manfredi JJ, Gu W, Aaronson SA. Ash2L enables P53-dependent apoptosis by favoring stable transcription pre-initiation complex formation on its pro-apoptotic target promoters. Oncogene. 2015;34(19):2461–70. https://doi.org/10.1038/onc.2014.198.
- Li Z. CD133: a stem cell biomarker and beyond. Exp Hematol Oncol. 2013;2(1):17. https://doi.org/10.1186/2162-3619-2-17.
- Paprocka M, Krawczenko A, Dus D, Kantor A, Carreau A, Grillon C, et al. CD133 positive progenitor endothelial cell lines from human cord blood. Cytom Part A. 2011;79(8):594–602. https://doi.org/10.1002/cyto.a.21092.
- Nishimura-Sakurai Y, Sakamoto N, Mogushi K, Nagaie S, Nakagawa M, Itsui Y, et al. Comparison of HCV-associated gene expression and cell signaling pathways in cells with or without HCV replicon and in replicon-cured cells. J Gastroenterol. 2010;45(5):523–36. https://doi.org/10.1007/s00535-009-0162-3.
- Zha K, Li X, Yang Z, Tian G, Sun Z, Sui X, et al. Heterogeneity of mesenchymal stem cells in cartilage regeneration: from characterization to application. NPJ Regen Med. 2021;6(1):14. https:// doi.org/10.1038/s41536-021-00122-6.
- Koyama N, Okubo Y, Nakao K, Osawa K, Fujimura K, Bessho K. Pluripotency of mesenchymal cells derived from synovial fluid in patients with temporomandibular joint disorder. Life Sci. 2011;89(19–20):741–7. https://doi.org/10.1016/j.lfs.2011.09.005.
- Wallace TM, Levy JC, Matthews DR. Use and abuse of HOMA modeling. Diabetes Care. 2004;27(6):1487–95. https://doi.org/10. 2337/diacare.27.6.1487.
- Venkatesan V, Madhira SL, Malakapalli VM, Chalasani M, Shaik SN, Seshadri V, et al. Obesity, insulin resistance, and metabolic syndrome: a study in WNIN/Ob rats from a pancreatic perspective. Biomed Res Int. 2013;2013: 617569. https://doi.org/10.1155/ 2013/617569.
- Samuel VT, Petersen KF, Shulman GI. Lipid-induced insulin resistance: unravelling the mechanism. Lancet (London, England). 2010;375(9733):2267–77. https://doi.org/10.1016/s0140-6736(10)60408-4.
- DeFronzo RA, Tripathy D. Skeletal muscle insulin resistance is the primary defect in type 2 diabetes. Diabetes Care. 2009;32(Suppl 2):S157-63. https://doi.org/10.2337/dc09-S302.
- Asghar A, Sheikh N. Role of immune cells in obesity induced low grade inflammation and insulin resistance. Cell Immunol. 2017;315:18–26. https://doi.org/10.1016/j.cellimm.2017.03.001.
- 53. Fève B, Bastard JP. The role of interleukins in insulin resistance and type 2 diabetes mellitus. Nat Rev Endocrinol. 2009;5(6):305–11. https://doi.org/10.1038/nrendo.2009.62.

- 54. Sell H, Habich C, Eckel J. Adaptive immunity in obesity and insulin resistance. Nat Rev Endocrinol. 2012;8(12):709–16. https://doi.org/10.1038/nrendo.2012.114.
- Frydrych LM, Bian G, O'Lone DE, Ward PA, Delano MJ. Obesity and type 2 diabetes mellitus drive immune dysfunction, infection development, and sepsis mortality. J Leukoc Biol. 2018;104(3):525–34. https://doi.org/10.1002/jlb.5vmr0118-021rr.
- Bandaru P, Rajkumar H, Nappanveettil G. Altered or impaired immune response to hepatitis B vaccine in WNIN/GR-Ob rat: an obese rat model with impaired glucose tolerance. ISRN Endocrinol. 2011;2011: 980105. https://doi.org/10.5402/2011/980105.
- Bandaru P, Rajkumar H, Nappanveettil G. Altered or impaired immune response upon vaccination in WNIN/Ob rats. Vaccine. 2011;29(16):3038–42. https://doi.org/10.1016/j.vaccine.2011.01. 107
- Lv FJ, Tuan RS, Cheung KM, Leung VY. Concise review: the surface markers and identity of human mesenchymal stem cells. Stem Cells (Dayton, Ohio). 2014;32(6):1408–19. https://doi.org/ 10.1002/stem.1681.
- Liu Y, Han ZP, Zhang SS, Jing YY, Bu XX, Wang CY, et al. Effects of inflammatory factors on mesenchymal stem cells and their role in the promotion of tumor angiogenesis in colon cancer. J Biol Chem. 2011;286(28):25007–15. https://doi.org/10.1074/ jbc.M110.213108.
- Odegaard JI, Chawla A. Alternative macrophage activation and metabolism. Annu Rev Pathol. 2011;6:275–97. https://doi.org/10. 1146/annurev-pathol-011110-130138.
- 61. Xie Z, Hao H, Tong C, Cheng Y, Liu J, Pang Y, et al. Human umbilical cord-derived mesenchymal stem cells elicit macrophages into an anti-inflammatory phenotype to alleviate insulin resistance in type 2 diabetic rats. Stem Cells (Dayton, Ohio). 2016;34(3):627–39. https://doi.org/10.1002/stem.2238.
- 62. Sun X, Hao H, Han Q, Song X, Liu J, Dong L, et al. Human umbilical cord-derived mesenchymal stem cells ameliorate insulin resistance by suppressing NLRP3 inflammasome-mediated inflammation in type 2 diabetes rats. Stem Cell Res Ther. 2017;8(1):241. https://doi.org/10.1186/s13287-017-0668-1.
- Wang Y, Chen X, Cao W, Shi Y. Plasticity of mesenchymal stem cells in immunomodulation: pathological and therapeutic implications. Nat Immunol. 2014;15(11):1009–16. https://doi.org/10. 1038/ni 3002.
- 64. von Bahr L, Batsis I, Moll G, Hägg M, Szakos A, Sundberg B, et al. Analysis of tissues following mesenchymal stromal cell therapy in humans indicates limited long-term engraftment and no ectopic tissue formation. Stem Cells (Dayton, Ohio). 2012;30(7):1575–8. https://doi.org/10.1002/stem.1118.
- Mäkelä T, Takalo R, Arvola O, Haapanen H, Yannopoulos F, Blanco R, et al. Safety and biodistribution study of bone marrowderived mesenchymal stromal cells and mononuclear cells and the impact of the administration route in an intact porcine model. Cytotherapy. 2015;17(4):392–402. https://doi.org/10.1016/j.jcyt. 2014.12.004.
- Hamidian Jahromi S, Davies JE. Concise review: skeletal muscle as a delivery route for mesenchymal stromal cells. Stem Cells Transl Med. 2019;8(5):456–65. https://doi.org/10.1002/sctm. 18-0208.
- Estrada EJ, Valacchi F, Nicora E, Brieva S, Esteve C, Echevarria L, et al. Combined treatment of intrapancreatic autologous bone marrow stem cells and hyperbaric oxygen in type 2 diabetes mellitus. Cell Transplant. 2008;17(12):1295–304. https://doi.org/10.3727/096368908787648119.
- Bhansali A, Upreti V, Khandelwal N, Marwaha N, Gupta V, Sachdeva N, et al. Efficacy of autologous bone marrow-derived stem cell transplantation in patients with type 2 diabetes mellitus. Stem Cells Dev. 2009;18(10):1407–16. https://doi.org/10.1089/ scd.2009.0164.



- Bhansali A, Asokumar P, Walia R, Bhansali S, Gupta V, Jain A, et al. Efficacy and safety of autologous bone marrow-derived stem cell transplantation in patients with type 2 diabetes mellitus: a randomized placebo-controlled study. Cell Transplant. 2014;23(9):1075–85. https://doi.org/10.3727/096368913x665576.
- Liu X, Zheng P, Wang X, Dai G, Cheng H, Zhang Z, et al. A
 preliminary evaluation of efficacy and safety of Wharton's jelly
 mesenchymal stem cell transplantation in patients with type 2
 diabetes mellitus. Stem Cell Res Ther. 2014;5(2):57. https://doi.
 org/10.1186/scrt446.
- Bhansali S, Kumar V, Saikia UN, Medhi B, Jha V, Bhansali A, et al. Effect of mesenchymal stem cells transplantation on glycaemic profile & their localization in streptozotocin induced diabetic Wistar rats. Indian J Med Res. 2015;142(1):63–71. https://doi.org/ 10.4103/0971-5916.162116.
- Kong D, Zhuang X, Wang D, Qu H, Jiang Y, Li X, et al. Umbilical cord mesenchymal stem cell transfusion ameliorated hyperglycemia in patients with type 2 diabetes mellitus. Clin Lab. 2014;60(12):1969–76. https://doi.org/10.7754/clin.lab.2014. 140305
- Skyler JS, Fonseca VA, Segal KR, Rosenstock J. Allogeneic mesenchymal precursor cells in type 2 diabetes: a randomized,

- placebo-controlled, dose-escalation safety and tolerability pilot study. Diabetes Care. 2015;38(9):1742–9. https://doi.org/10.2337/dc14-2830.
- Wu Z, Cai J, Chen J, Huang L, Wu W, Luo F, et al. Autologous bone marrow mononuclear cell infusion and hyperbaric oxygen therapy in type 2 diabetes mellitus: an open-label, randomized controlled clinical trial. Cytotherapy. 2014;16(2):258–65. https:// doi.org/10.1016/j.jcyt.2013.10.004.
- 75. Bhansali S, Dutta P, Kumar V, Yadav MK, Jain A, Mudaliar S, et al. Efficacy of autologous bone marrow-derived mesenchymal stem cell and mononuclear cell transplantation in type 2 diabetes mellitus: a randomized, placebo-controlled comparative study. Stem Cells Dev. 2017;26(7):471–81. https://doi.org/10.1089/scd. 2016.0275.

Publisher's Note Springer Nature remains neutral with regard to jurisdictional claims in published maps and institutional affiliations.

